A MIXED-MODE GPS NETWORK PROCESSING APPROACH FOR DEFORMATION MONITORING APPLICATIONS

Volker Janssen and Chris Rizos

School of Surveying and Spatial Information Systems
The University of New South Wales
Sydney NSW 2052, Australia

ABSTRACT

The Global Positioning System (GPS) can be utilised in a wide range of deformation monitoring applications, such as the monitoring of active volcanoes, tectonic fault lines, landslides, ground subsidence, bridges, dams, high-rise buildings, etc. During the past few years a methodology has been developed for processing data collected by GPS networks consisting of a mixed set of single-frequency and dual-frequency receivers. The strategy is to deploy a few permanent, 'fiducial' GPS stations with dual-frequency, geodetic-grade receivers surrounding an 'inner' network of low-cost, single-frequency GPS receivers. Such a configuration offers considerable flexibility and cost savings for deformation monitoring applications, which require a dense spatial coverage of GPS stations, and where it is not possible, nor appropriate, to establish permanent GPS networks using dual-frequency instrumentation.

The basis of the processing methodology is to separate the dual-frequency, 'fiducial' station data processing from the baseline processing involving the inner (single-frequency) receivers located in the deformation zone. The data processing for the former is carried out using a modified version of the Bernese software, to generate a file of 'corrections' (analogous to Wide Area DGPS correction models for the distance dependent biases - primarily due to atmospheric refraction). These 'corrections' are then applied to the double-differenced phase observations from the inner receivers to improve the single-frequency baseline accuracies (primarily through empirical modelling of the residual atmospheric biases that otherwise would be neglected).

This configuration has been tested by simulating such a two-stage network using data collected by part of the Southern California Integrated GPS Network (SCIGN). Six sites forming an inner network of three GPS receivers surrounded by three 'fiducial' GPS receivers are used in this study. All sites are equipped with dual-frequency instrumentation, however, for most of the analysis the inner sites are treated as single-frequency stations by ignoring the observations made on L2. A description of the processing strategy, together with a discussion of the results is presented.

INTRODUCTION

The Global Positioning System (GPS) can be utilised in a wide range of deformation monitoring applications. The decreasing cost of GPS hardware, together with the increased reliability of the technology, facilitates such demanding applications as the monitoring of active volcanoes, tectonic fault lines, landslides, ground subsidence, bridges, dams, high-rise buildings, etc. GPS deformation measurements can be continuous, automatic, conducted in all weather conditions and provide three-dimensional positioning results. Higher computing power also means that the complex mathematics required to process GPS baselines can be easily handled in near real-time.

Deformation monitoring using GPS is usually carried out by installing and operating a local network of GPS receivers located on and around the deforming body. One of the first *continuous* GPS networks was established in March 1988 on the Izu Peninsula in central Japan to support earthquake prediction research. Daily observations of this network led to the first GPS measurements of surface deformation as they occurred. [**25**] reported that, "*We have, for the first time, used GPS fixed-point measurements to follow the evolution with time of the crustal movements; such measurements provide a continuous uninterrupted record of deformation.*" Numerous continuous networks of different size have since been established on skyscrapers [**17**], bridges [**2**, **29**], volcanoes [**6**] and tectonic fault lines [**27**, **3**, **10**].

However, these networks are very costly because they rely entirely on the use of high-quality dual-frequency instrumentation. In order to keep the cost of such a deformation monitoring system to a minimum, single-frequency GPS receivers need to be used. However, these cost savings come at a 'price'. Due to the use of only one frequency, the ionospheric delay cannot be accounted for directly. A single-frequency, carrier phase-tracking system is appropriate for small-scale continuous GPS networks if the baseline lengths are not longer than 10 kilometres. This 'rule-of-thumb' implies that the differential ionospheric and tropospheric delay between the two receivers is essentially zero, and therefore does not impact on the baseline result. Orbit bias over such short distances can also be ignored [**18**]. However, with the current solar sunspot cycle maximum, ionospheric disturbances have indeed corrupted baseline measurements over distances less than 10km, adversely affecting baseline repeatability [**12**]. It is therefore necessary to combine a single-frequency deformation monitoring network with a small number of dual-frequency receivers in order to account for these atmospheric effects. [**15**] reports on a single-frequency system for volcano deformation monitoring at the Long Valley Caldera, USA and Mt. Popocatepetl, Mexico, which is soon to be augmented with the addition of a small number of dual-frequency receivers for atmospheric modelling. [**9**] describe a mixed-mode approach to monitor landslides in the Austrian Alps.

In this paper a fiducial network of three dual-frequency GPS receivers surrounding the deformation zone is used to generate empirical 'correction terms' [**19**, **20**]. These double-differenced corrections are then applied to the data from the single-frequency baselines in the inner network to account for residual atmospheric biases. The ionospheric correction model proposed for this mixed-mode system and the data processing strategy are described, and experimental results are presented.

IONOSPHERIC CORRECTIONS

The ionosphere is that part of the Earth's atmosphere located at a height of approximately 50km–1000km above the surface and has a major effect on GPS signals travelling from the satellite to the receiver. The condition of the ionosphere is strongly related to the 11-year sunspot activity cycle. The most recent solar maximum occurred in 2000/2001 causing high ionospheric activity, and subsequently having a distinct impact on the data presented in this paper.

The ionosphere is most active in a band extending up to approximately 20° on either side of the geomagnetic equator. This is also one of the two regions where small-scale ionospheric disturbances (scintillations) mainly occur, the other being the high-latitude region close to the poles. Scintillations are short-term signal variations in amplitude and phase. In the equatorial region scintillations occur between approximately one hour after sunset until midnight [**14**] and should have disappeared by 3am local time [**13**]. The occurrence of scintillations also varies with the seasons. Between April and August they are less severe in the American, African and Indian longitude regions, but are at a maximum in the Pacific region, while the situation is reversed from September to March [**24**]. In mid-latitudes scintillations are rarely experienced, but Medium-Scale Travelling Ionospheric Disturbances (MSTIDs) occur frequently, mainly during daytime in the winter months, during periods of high solar activity, with a maximum around local noon [**28**].

While dual-frequency receivers can account for the ionospheric delay directly by the appropriate linear combination of measurements from both frequencies, single-frequency receivers do not have this option. For deformation monitoring applications, a network of three dual-frequency receivers surrounding the deformation zone can be

used to generate 'correction terms', which can then be applied to the single-frequency observations to account for these effects.

As described in [**7**], the fiducial network should ideally surround the inner single-frequency network leaving it in the centre of the triangle. Figure 1 shows the ideal network configuration where the triangles denote fiducial stations, while the dots indicate single-frequency sites.

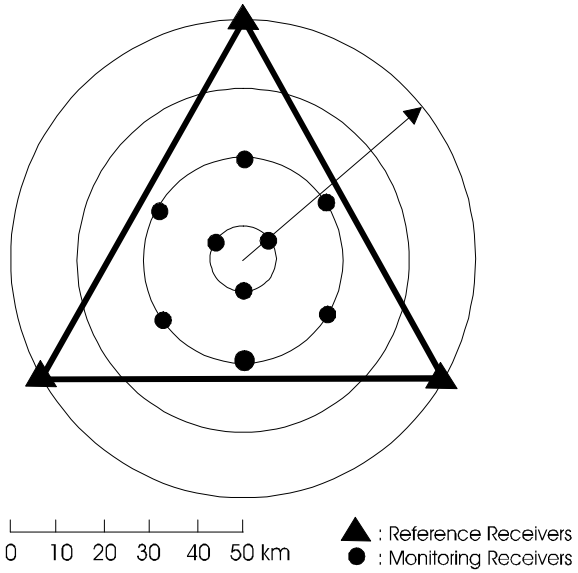

Fig. 1. Ideal network configuration of a mixed-mode GPS deformation monitoring network

A linear combination model has been proposed by [**8**] and [**7**], which can account for orbit bias and ionospheric delay, as well as mitigate tropospheric delay, multipath and measurement noise across the network. Data from the fiducial GPS reference station network can be used to derive empirical corrections to the double-differenced carrier phase data formed between the stations of the inner network. The procedure is described in [**4**] and summarised below.

The double-differenced carrier phase observable can be written as [**4**]:

$$\nabla\Delta\phi = \nabla\Delta\rho + \nabla\Delta d\rho + \lambda \cdot \nabla\Delta N - \nabla\Delta d_{ion} + \nabla\Delta d_{trop} + \nabla\Delta d^{\varphi}_{mp} + \varepsilon_{\nabla\Delta\phi} \qquad (1)$$

where $\nabla\Delta$ = double-difference operator
ϕ = carrier phase observation in units of metres
ρ = vector between receiver station and satellite
$d\rho$ = effect of satellite ephemeris error on a particular receiver-satellite vector
λ = wavelength of the carrier phase
N = integer ambiguity for a particular satellite-receiver pair
d_{ion}, d_{trop}, d^{φ}_{mp} = ionospheric delay, tropospheric delay, multipath effect
$\varepsilon_{\nabla\Delta\phi}$ = carrier phase observation noise for a particular one-way observation

Assume that the number of GPS reference stations is three. For a baseline between one of these reference stations and a single-frequency user receiver (denoted by u) located inside the fiducial triangle, the above equation can then be written in the form of a linear combination [**7**]:

$$\nabla\Delta\phi_{u,3} - \left[\alpha_1 \cdot V_{1,3} + \alpha_2 \cdot V_{2,3}\right] = \nabla\Delta\rho_{u,3} + \lambda \cdot \nabla\Delta N_{u,3} + \varepsilon_{\nabla\Delta\phi_{u,3}} \qquad (2)$$

The parameters α_i refer to the position of the user receiver inside the fiducial triangle and can be determined based on the conditions given in [**8**] and [**30**]:

$$\sum_{i=1}^{3}\alpha_i = 1, \quad \sum_{i=1}^{3}\alpha_i \cdot \left(\vec{X}_u - \vec{X}_i\right) = 0 \text{ and } \sum_{i=1}^{3}\alpha_i^2 = \min \qquad (3)$$

where $\vec{X}_u$ = user station position vector and $\vec{X}_i$ = reference station position vector.

The residual vectors are formed from the double-differenced observations between reference stations 1 & 3 and 2 & 3:

$$\begin{aligned} V_{1,3} &= \nabla\Delta\phi_{1,3} - \nabla\Delta N_{1,3} - \nabla\Delta\rho_{1,3} \\ V_{2,3} &= \nabla\Delta\phi_{2,3} - \nabla\Delta N_{2,3} - \nabla\Delta\rho_{2,3} \end{aligned} \qquad (4)\ \&\ (5)$$

The correction term $\left[\alpha_1 \cdot V_{1,3} + \alpha_2 \cdot V_{2,3}\right]$ can now be determined. If the baseline between two GPS stations j and k of the inner network is considered, the linear combination can be written as:

$$\nabla\Delta\phi_{k,j} - \left[\alpha_1^{k,j} \cdot V_{1,3} + \alpha_2^{k,j} \cdot V_{2,3}\right] = \nabla\Delta\rho_{k,j} + \lambda \cdot \nabla\Delta N_{k,j} + \varepsilon_{k,j} \qquad (6)$$

where $\alpha_i^{k,j}$ = difference in the α_i value for stations j and k.

By forming the double-differenced observables between the inner single-frequency receivers, and using the residual vectors generated from the fiducial reference stations, the inner stations' coordinates can be determined without the need to use any GPS reference station observations at all.

Therefore, holding one fiducial site fixed, the baselines to the other two sites are processed and 'correction terms' are obtained for both baselines. These are then scaled according to the position of the inner stations inside the fiducial triangle to generate double-differenced corrections for the inner baselines.

The nature of the empirically-derived double-differenced 'correction terms' has been investigated by [**12**]. A range of GPS data sets were processed incorporating a variety of baseline lengths, different geographical locations and different periods of sunspot activity (and hence ionospheric conditions). The standard deviation of the double-differenced 'correction terms' was found to increase linearly with increasing baseline length. The rate of increase was much more severe under solar maximum conditions as opposed to periods of low solar activity. This suggests that long baselines between reference stations might not be capable of generating reliable corrections under these conditions. However, the magnitude of these biases is not entirely a function of distance, hence it is difficult to predict what should be the dimensions of the reference station network that would faithfully model the distance-dependent biases. The geographic location of the network is certainly another contributing factor, as the ionospheric effects for GPS sites in the equatorial region are much larger compared to mid-latitude sites.

SINGLE-FREQUENCY DATA PROCESSING

A single-frequency version of the Baseline software package developed at UNSW is used to process the inner network. For deformation monitoring applications multi-baseline processing strategies should be used because all baselines are then computed together, taking into account the between-baseline correlations which arise from observing a GPS network simultaneously [**5**]. For continuous deformation monitoring applications, a near-real-time, epoch-by-epoch solution is desired in order to detect movements over a short period of time. In a number of deformation monitoring applications, such as local networks around active volcanoes or dams, the deforming body itself will obstruct part of the sky. If the usual base-station / base-satellite approach is used in the data processing, only the common satellites are considered, resulting in the number of possible double differences being comparatively low, hence a lot of potentially valuable information can be lost. As described in [**11**], the Baseline software utilises a procedure to optimise the number of double-differenced observations used in the data processing. This method considers satellites that are visible from a small number of network stations only. Hence, the number of independent double-differenced observables can be maximised in order to generate a more accurate and reliable solution. The data processing approach determines the receiver-to-satellite connections for each site of the network. A maximum set of independent double-differenced combinations is then computed using vector space methods and the geometric characterisations of Boolean matrices, as suggested by [**22**].

EXPERIMENTAL DATA

Data from the Southern California Integrated GPS Network (SCIGN) [**10**, **23**] was used to investigate the performance of such a network configuration. Figure 2 shows the location of the GPS sites, which are all equipped with dual-frequency receivers. The part of the network used here contains an outer network of three sites (FXHS, FMTP, QHTP) surrounding an inner network of three sites (CSN1, OAT2, CMP9). The outer sites were used as fiducial GPS reference stations, indicated by triangles in Figure 2, while the inner sites (indicated by circles) were mainly used as single-frequency stations by ignoring the observations taken on L2. The data was collected under solar maximum conditions using an observation rate of 30s on three consecutive days from 8-10 August 2000 (DOY 221-223).

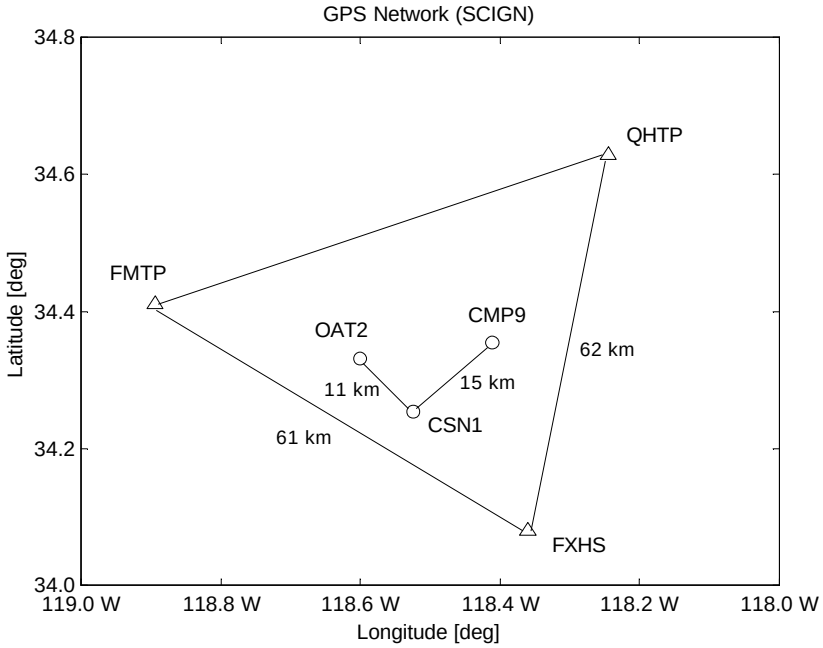

Fig. 2. Part of the GPS network in California (SCIGN)

The WGS-84 coordinates of the GPS network stations are shown in Table 1. These coordinates were obtained using the Scripps Coordinate Update Tool (SCOUT) provided by the Scripps Orbit and Permanent Array Center (SOPAC) [**26**]. This service computes the coordinates of a user station by using the three closest located SCIGN reference sites, and the precise ephemerides. The coordinates in Table 1 were obtained by taking the mean of five 24-hour solutions on successive days (average baseline length 6-18km). The inner network sites were particularly chosen to simulate conditions present in a GPS volcano deformation monitoring network where significant height differences between the base station on the foot of the volcano and the monitoring 'slave' stations on the flanks of the volcano typically occur.

Tab. 1. *WGS-84 coordinates of the GPS network stations (Figure 2)*

Site	FMHS	FMTP	QHTP
X [m]	-2511943.6388	-2545459.7204	-2486712.3456
Y [m]	-4653606.7722	-4612207.1586	-4629002.0822
Z [m]	3553873.9778	3584252.1200	3604537.5090
Latitude (N)	34° 04' 50.1730''	34° 24' 35.5071''	34° 37' 43.2475''
Longitude (W)	118° 21' 34.1088''	118° 53' 38.9045''	118° 14' 41.3211''
Height [m]	33.319	362.805	863.039
Site	CSN1	OAT2	CMP9
X [m]	-2520225.8551	-2524553.6438	-2508505.9552
Y [m]	-4637082.4402	-4630094.2566	-4637175.0256
Z [m]	3569875.3624	3577352.1138	3579499.8619
Latitude (N)	34° 15' 12.7752''	34° 19' 47.6064''	34° 21' 11.4434''
Longitude (W)	118° 31' 25.7116''	118° 36' 04.9555''	118° 24' 41.1177''
Height [m]	261.443	1112.587	1138.042

IONOSPHERIC CORRECTIONS FOR THE FIDUCIAL BASELINES

Processing the dual-frequency data with a modified version of the Bernese software, ionospheric L1 correction terms were determined for four baselines on three successive days. The baselines FXHS-FMTP (61km) and FXHS-QHTP (62km) were used as fiducial reference baselines. For comparison, corrections were also obtained for the inner baselines CSN1-OAT2 (11km) and CSN1-CMP9 (15km) using observations made on both frequencies. Table 2 shows several parameters characterising the correction terms, i.e. the minimum, maximum and mean corrections, their standard deviations and the number of double-differences involved. Figures 3-5 show the double-differenced corrections obtained for the fiducial baselines on L1 for three consecutive 24-hour observation sessions, while Figures 6-8 show the corrections obtained for the inner baselines. It can be seen that ionospheric activity in mid-latitudes is a daytime phenomenon with most of the ionospheric activity occurring between local sunrise and sunset. Obviously the ionosphere was a little less active on day 222 compared to days 221 and 223. The correction terms for both fiducial baselines show a similar pattern, indicating that the ionospheric conditions have been rather homogeneous across the network during the time of observation. The magnitude of the corrections for the fiducial baselines reaches values of a few cycles, indicating that the ionospheric effect is significant. Due to the shorter baseline length, the corrections for the inner baselines are smaller than those obtained for the fiducial baselines.

Tab. 2. *Double-differenced L1 corrections for different baselines*

Baseline	D [km]	min [m]	max [m]	mean [m]	STD [m]	#DD
SCIGN: DOY 221 (L1)						
FXHS-FMTP	61	-0.47601	0.57315	0.00893	0.13664	15747
FXHS-QHTP	62	-0.76940	0.68799	0.00452	0.16120	15722
CSN1-OAT2	11	-0.14378	0.12188	0.00043	0.03173	15884
CSN1-OAT2*	11	-0.09892	0.11910	0.00169	0.02619	15613
CSN1-CMP9	15	-1.25630	0.83254	0.00547	0.05508	15206
CSN1-CMP9*	15	-0.17262	0.11415	-0.00013	0.03622	15613
SCIGN: DOY 222 (L1)						
FXHS-FMTP	61	-0.52535	0.46483	-0.00341	0.13336	14303
FXHS-QHTP	62	-0.44155	0.43618	-0.00032	0.12339	14254
CSN1-OAT2	11	-0.11631	0.10590	0.00489	0.02884	14337
CSN1-OAT2*	11	-0.10111	0.07784	-0.00047	0.02399	14182
CSN1-CMP9	15	-0.36008	0.48812	0.00401	0.04750	13868
CSN1-CMP9*	15	-0.10325	0.09635	0.00045	0.02937	14182
SCIGN: DOY 223 (L1)						
FXHS-FMTP	61	-0.63624	0.88364	0.00338	0.15906	15181
FXHS-QHTP	62	-0.85886	0.74558	-0.01725	0.14455	15120
CSN1-OAT2	11	-0.53362	0.37751	-0.00137	0.03578	15271
CSN1-OAT2*	11	-0.12634	0.13803	-0.00019	0.02767	15044
CSN1-CMP9	15	-1.12856	0.83593	-0.00229	0.06732	14669
CSN1-CMP9*	15	-0.18709	0.12648	-0.00507	0.03771	15044
* calculated using α values						

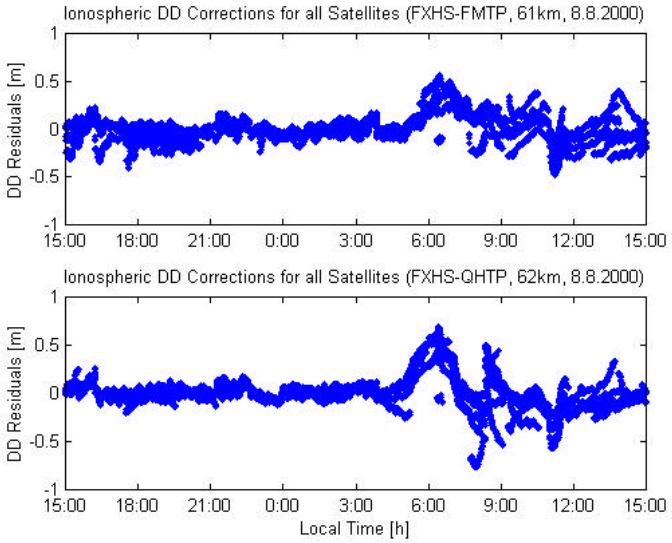

Fig. 3. Double-differenced L1 corrections for the fiducial baselines (DOY 221)

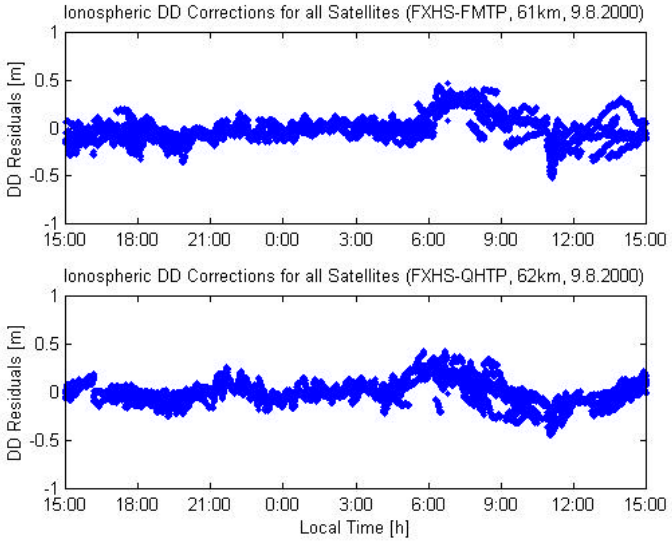

Fig. 4. Double-differenced L1 corrections for the fiducial baselines (DOY 222)

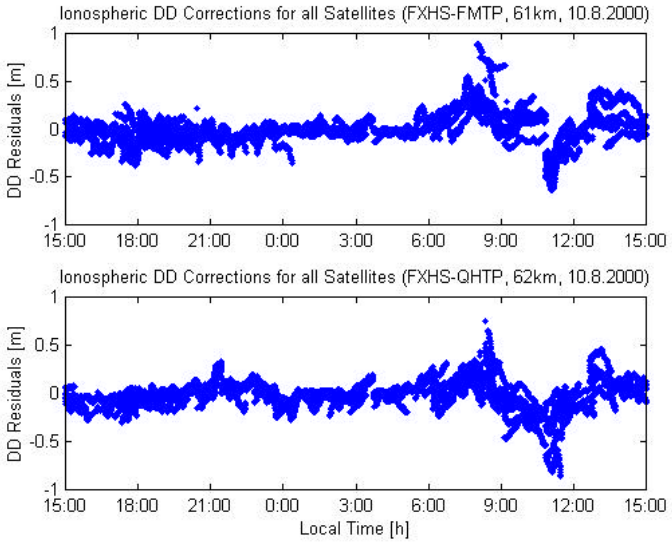

Fig. 5. Double-differenced L1 corrections for the fiducial baselines (DOY 223)

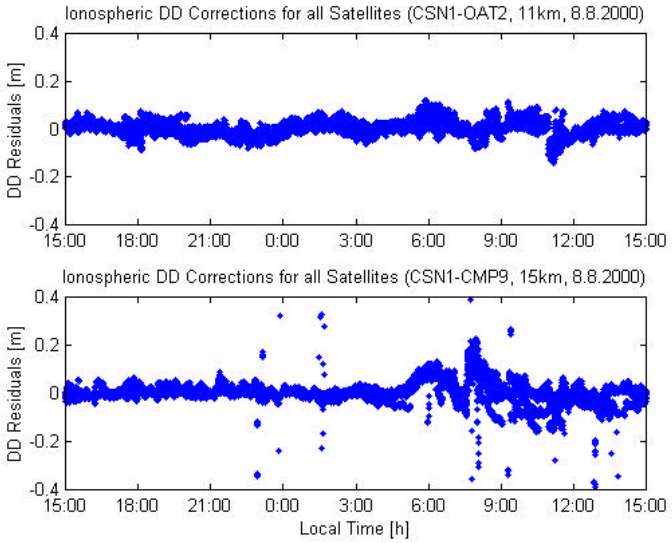

Fig. 6. Double-differenced L1 corrections for the inner baselines (DOY 221)

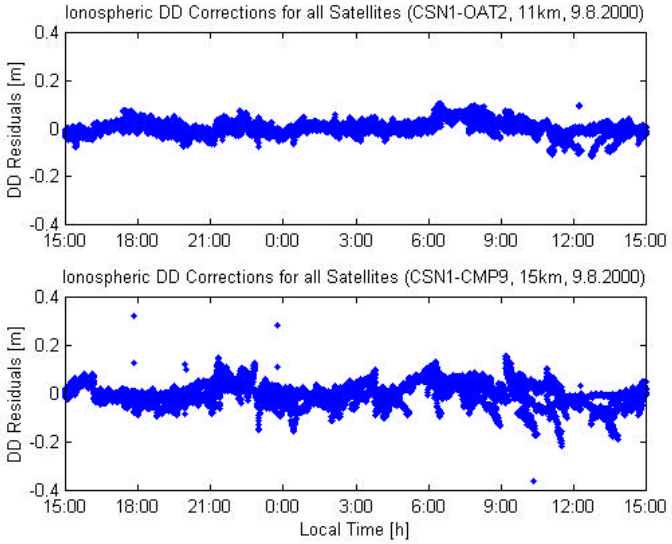

Fig. 7. Double-differenced L1 corrections for the inner baselines (DOY 222)

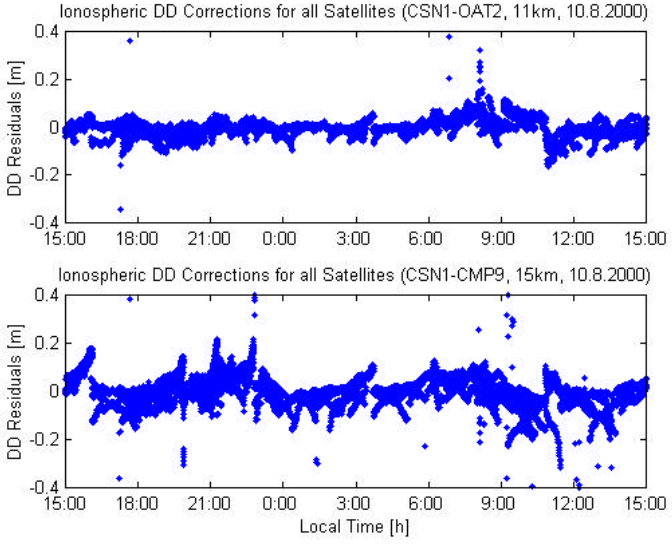

Fig. 8. Double-differenced L1 corrections for the inner baselines (DOY 223)

IONOSPHERIC CORRECTIONS FOR THE INNER BASELINES

According to the procedure described earlier, the α values were derived in order to relate the position of the inner network sites to the fiducial baselines. Table 3 lists the α values obtained for the inner GPS sites, α_1 and α_2 indicating the values corresponding to the fiducial baselines FXHS-FMTP and FXHS-QHTP respectively.

Tab. 3. *a values obtained for the inner GPS network stations*

Site	α_1	α_2
CSN1	0.332228	0.115962
OAT2	0.487210	0.162147
CMP9	0.180552	0.388863

The L1 correction terms for the inner baselines can then be determined by forming the linear combination according to equation (6). In order to form this linear combination, the correction files have been modified to ensure the same number of double-differenced correction terms with matching receiver-satellite pairs for both fiducial baselines. Hence, the double-differenced correction terms for the inner baselines could be derived in two different ways. Firstly, as described in the previous section, the corrections were determined directly using dual-frequency data and the modified Bernese software (Figures 6-8). Secondly, they were obtained indirectly by forming a linear combination of the corrections for the fiducial baselines using the α values (Figures 9-11). Several parameters characterising these correction terms are shown in Table 2 (indicated by asterisks). It can clearly be seen that the results are very similar. The corrections generated using the proposed method are a little smoother and do not show 'outliers' present in the directly determined correction terms. They certainly model the main characteristics of the correction terms very well. This proves that the proposed procedure indeed delivers the correct correction terms for the inner baselines.

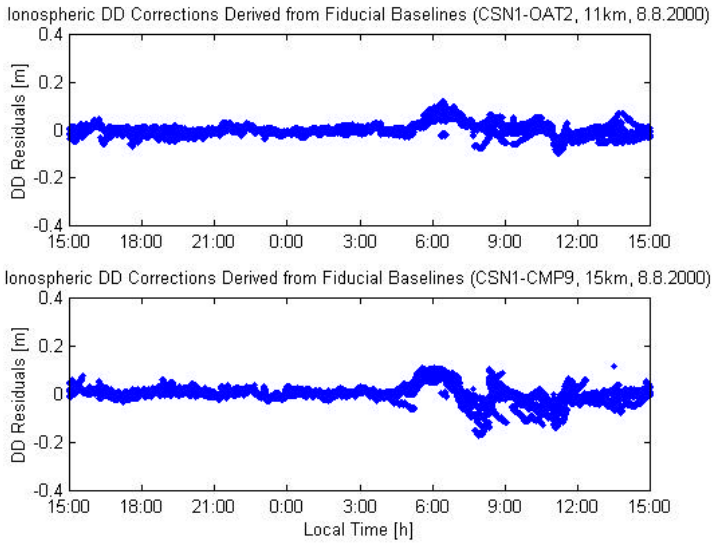

Fig. 9. Double-differenced L1 corrections for the inner baselines obtained using α values (DOY 221)

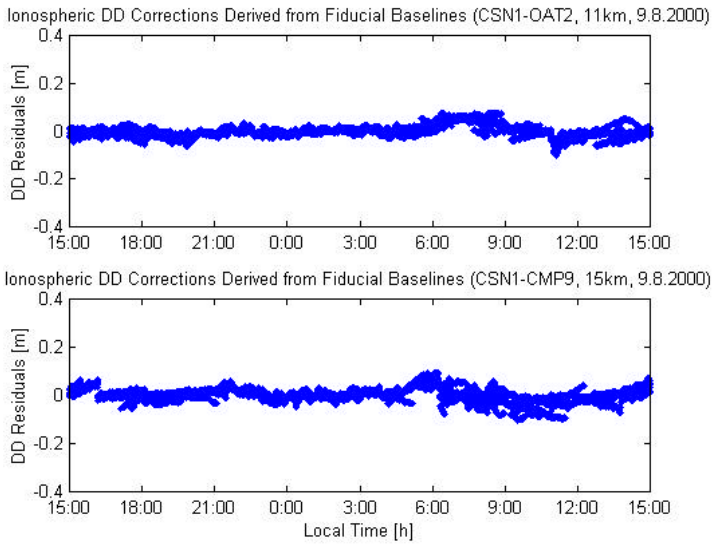

Fig. 10. Double-differenced L1 corrections for the inner baselines obtained using α values (DOY 222)

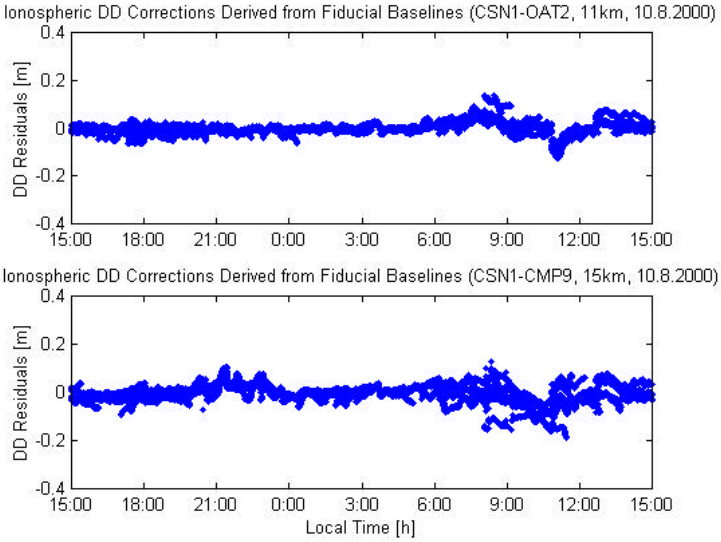

Fig. 11. Double-differenced L1 corrections for the inner baselines obtained using α values (DOY 223)

BASELINE RESULTS

The Baseline software developed at UNSW is used to process the inner baselines in single-frequency mode with and without using ionospheric correction terms. It can readily be assumed that no ground deformation has taken place during the time of observation. Hence, the baseline repeatability gives a good indication of the accuracy that can be achieved with the method described in this paper. Figures 12-17 show the results obtained for the inner baselines using the Baseline software without applying ionospheric corrections, while Figures 18-23 show the results obtained by applying ionospheric corrections. The graphs show the Easting, Northing and Height components over a 24-hour period on three successive days, each dot representing a single-epoch solution. The standard deviation of each component is also given. In both cases the Saastamoinen model was used to account for the tropospheric bias, as recommended by [**16**].

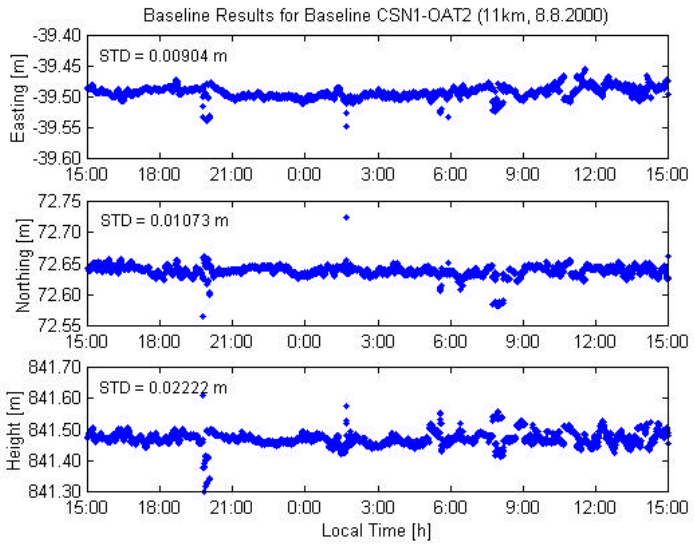

Fig. 12. Results for inner baseline CSN1-OAT2 not using ionospheric corrections (DOY 221)

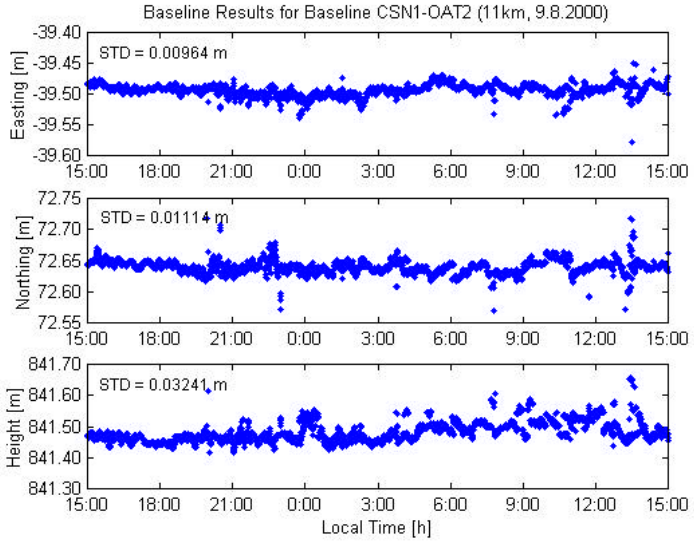

Fig. 13. Results for inner baseline CSN1-OAT2 not using ionospheric corrections (DOY 222)

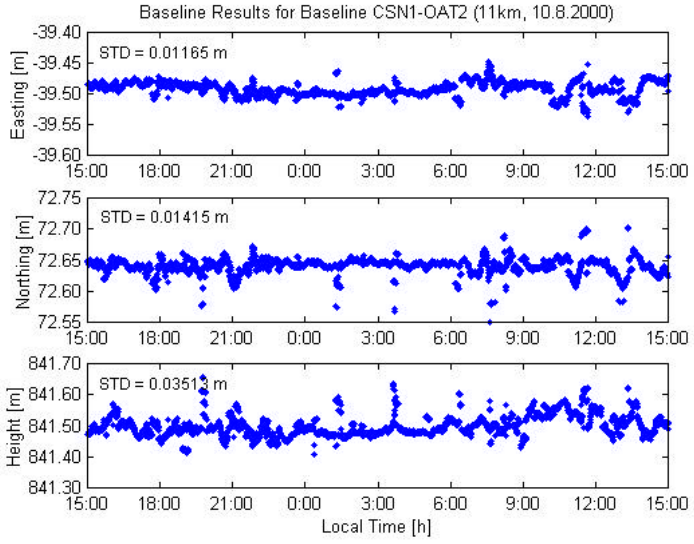

Fig. 14. Results for inner baseline CSN1-OAT2 not using ionospheric corrections (DOY 223)

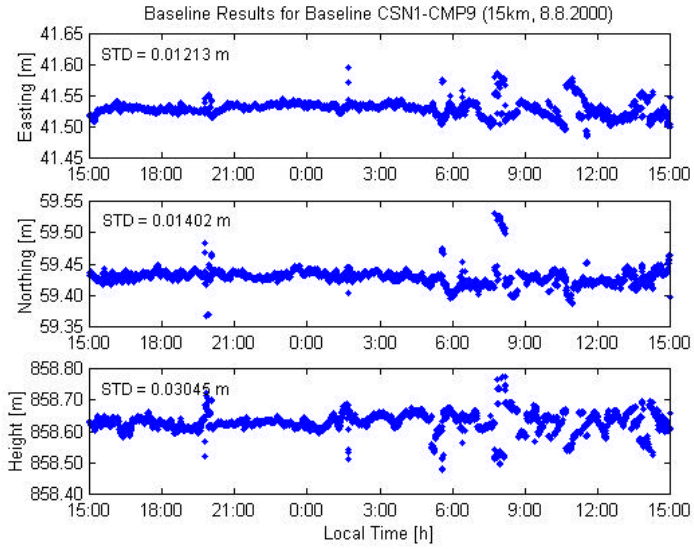

Fig. 15. Results for inner baseline CSN1-CMP9 not using ionospheric corrections (DOY 221)

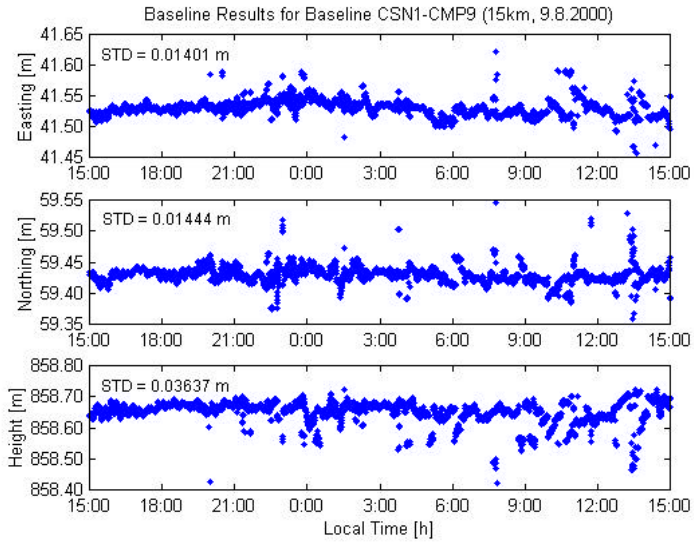

Fig. 16. Results for inner baseline CSN1-CMP9 not using ionospheric corrections (DOY 222)

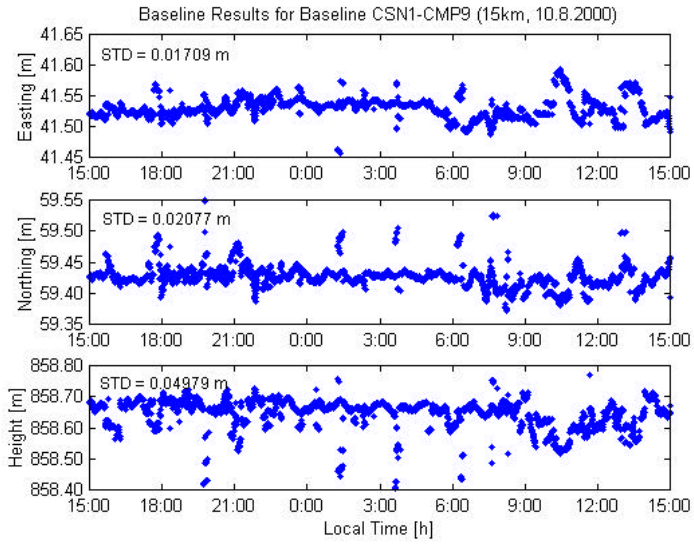

Fig. 17. Results for inner baseline CSN1-CMP9 not using ionospheric corrections (DOY 223)

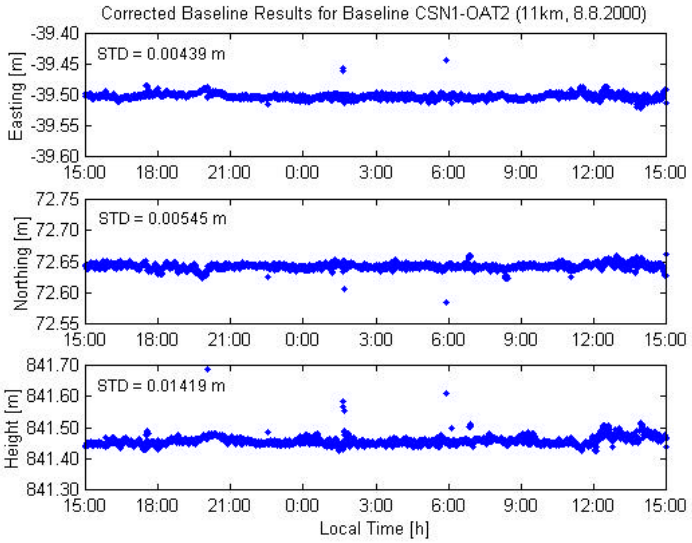

Fig. 18. Results for inner baseline CSN1-OAT2 applying ionospheric corrections (DOY 221)

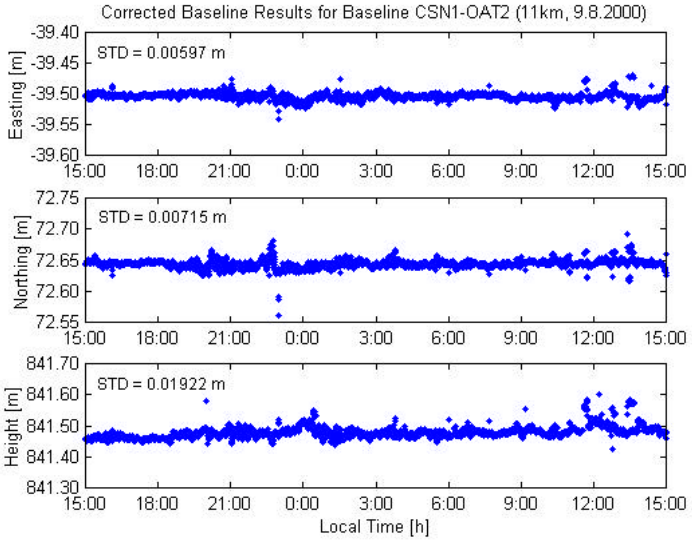

Fig. 19. Results for inner baseline CSN1-OAT2 applying ionospheric corrections (DOY 222)

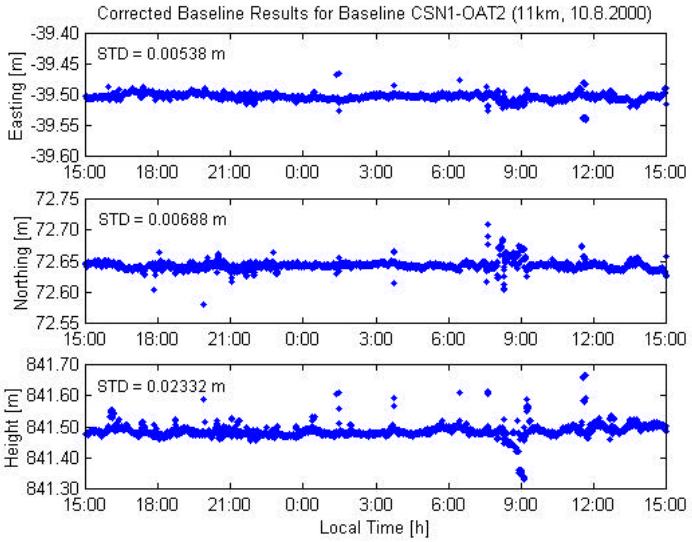

Fig. 20. Results for inner baseline CSN1-OAT2 applying ionospheric corrections (DOY 223)

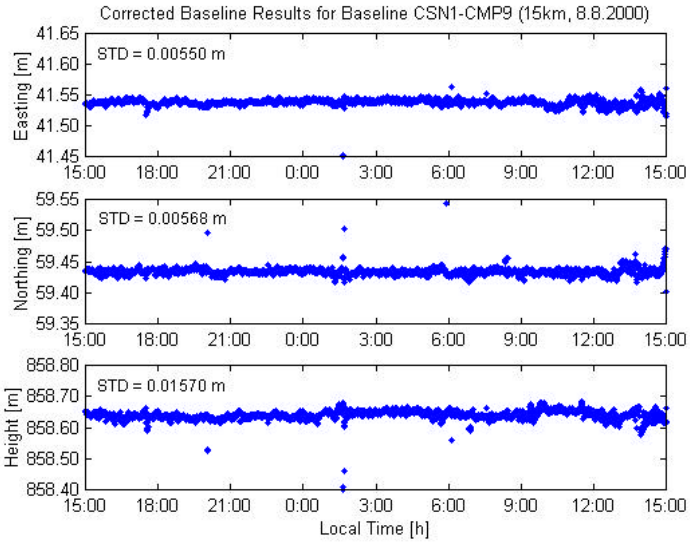

Fig. 21. Results for inner baseline CSN1-CMP9 applying ionospheric corrections (DOY 221)

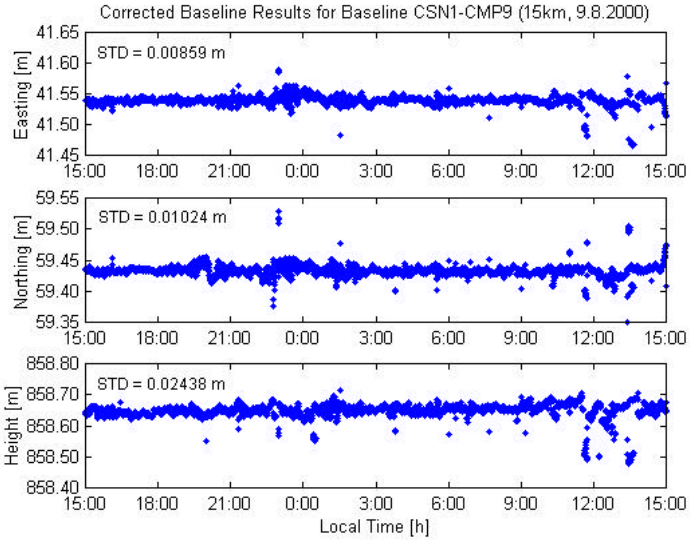

Fig. 22. Results for inner baseline CSN1-CMP9 applying ionospheric corrections (DOY 222)

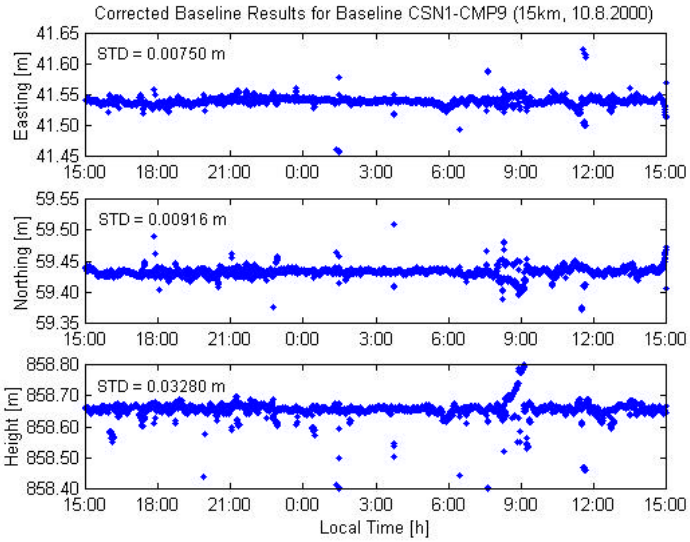

Fig. 23. Results for inner baseline CSN1-CMP9 applying ionospheric corrections (DOY 223)

Table 4 lists the standard deviations (STD) of the results obtained for the inner baselines using the two different processing methods (not applying corrections versus applying corrections) on three successive days. Comparing Figures 12-17 and Figures 18-23, and taking note of the information given in Table 4, it is evident that the baseline results are improved significantly by applying the correction terms. On average, the standard deviation of the baseline results has been reduced by almost 50% in the horizontal and almost 40% in the vertical component (Table 5). Using the proposed processing strategy, standard deviations of less than 1cm horizontally and 1.5-3cm vertically have been achieved for a single-epoch baseline solution (Table 4).

For baselines involving a significant difference in station altitude, e.g. in GPS volcano deformation monitoring networks, the accuracy could be further improved by estimating an additional residual relative zenith delay parameter to account for the tropospheric bias. Among others, [**1**] and [**21**] state that global troposphere models alone are not sufficient in this case and the relative tropospheric delay should be estimated.

Tab. 4. *Standard deviations of the inner baseline components on days 221-223*

	Day 221, no corr.	Day 221, corr.	Day 222, no corr.	Day 222, corr.	Day 223, no corr.	Day 223, corr.
Baseline CSN1-OAT2						
Easting [m]	0.00904	0.00439	0.00964	0.00597	0.01165	0.00538
Northing [m]	0.01073	0.00545	0.01114	0.00715	0.01415	0.00688
Height [m]	0.02222	0.01419	0.03241	0.01922	0.03513	0.02332
Baseline CSN1-CMP9						
Easting [m]	0.01213	0.00550	0.01401	0.00859	0.01709	0.00750
Northing [m]	0.01402	0.00568	0.01444	0.01024	0.02077	0.00916
Height [m]	0.03045	0.01570	0.03637	0.02438	0.04979	0.03280

Tab. 5. *Average improvement in the STD for both baselines on days 221-223*

Baseline	DOY	Easting [%]	Northing [%]	Height [%]
CSN1-OAT2 (11km)	221	51.4	49.2	36.1
	222	38.1	35.8	40.7
	223	53.8	51.4	33.6
CSN1-CMP9 (15km)	221	54.7	59.5	48.4
	222	38.7	29.1	33.0
	223	56.1	55.9	34.1
Average [%]		49	47	38

CONCLUDING REMARKS

A procedure to process a mixed-mode GPS network for deformation monitoring applications has been described. Single-frequency GPS observations have been enhanced using empirical corrections obtained from a fiducial network of dual-frequency reference stations surrounding the inner single-frequency network. This method accounts for the ionospheric bias that otherwise would have been neglected if using single-frequency instrumentation only. Data from the SCIGN network have been

used to simulate such a network configuration in order to investigate the impact of the proposed processing strategy on baseline results.

The generated correction terms have highlighted that the ionosphere has a significant effect on the GPS baseline results. This effect should not be neglected if it is desired to detect deformational signals with single-frequency instrumentation at a high-accuracy level, even for short baselines in mid-latitudes with rather homogeneous ionospheric conditions across the network.

The double-differenced correction terms for the inner baselines were derived in two different ways, directly using dual-frequency data and indirectly using the modelling approach. It was shown that the correction generation algorithm proposed in this paper successfully models the correction terms for the inner (single-frequency) baselines.

The single-frequency baseline repeatability has clearly been improved by applying the empirical correction terms. The standard deviation of the baseline results has been reduced by almost 50% in the horizontal and almost 40% in the vertical component. Standard deviations of less than 1cm horizontally and 1.5-3cm vertically have been achieved for a single-epoch baseline solution.

The approach of processing a mixed-mode GPS network described in this paper is a cost-effective and accurate tool for deformation monitoring suitable for a variety of applications.

ACKNOWLEDGEMENTS

SCIGN and its sponsors, the W.M. Keck Foundation, the National Aeronautics & Space Administration (NASA), the National Science Foundation (NSF), the U.S. Geological Survey (USGS) and the Southern California Earthquake Center (SCEC), are thanked for providing the data used in this analysis. The first author is supported in his Ph.D. studies by an International Postgraduate Research Scholarship (IPRS) and funding from the Australian Research Council (ARC).

References

1. Abidin, H.Z., Meilano, I., Suganda, O.K., Kusuma, M.A., Muhardi, D., Yolanda, O., Setyadji, B., Sukhyar R., Kahar J. and Tanaka, T., 1998. Monitoring the Deformation of Guntur Volcano Using Repeated GPS Survey Method, *Proc. XXI Int. Congress of FIG, Commission 5*, Brighton, UK, 19-25 July, 153-169.
2. Ashkenazi, V., Dodson, A.H., Moore, T. and Roberts, G.W., 1997. Monitoring the Movements of Bridges by GPS, *Proc. ION GPS-92*, Kansas City, Missouri, 16-19 September, 1165-1172.
3. Bock, Y., Wdowinski, S., Fang, P., Zhang, J., Williams, S., Johnson, H., Behr, J., Genrich, J., Dean, J., van Domselaar, M., Agnew, D., Wyatt, F., Stark, K., Oral, B., Hudnut, K., King, R., Herring, T., Dinardo, S., Young, W., Jackson, D. and Gurtner, W., 1997. Southern California Permanent GPS Array: Continuous Measurements of Regional Crustal Deformation Between the 1992 Landers and 1994 Northridge Earthquakes, *Journal of Geophysical Research*, 102(B8), 18013-18033.
4. Chen, H.Y., Rizos, C. and Han, S., 1999. Rapid Static, Medium-Range GPS Positioning Techniques for Geodynamic Applications, *Proc. 4th Australasian Symp. on Satellite Navigation Technology & Applications*, Brisbane, Australia, 20-23 July, Paper 49, 12pp.

5. Craymer, M.R. and Beck, N., 1992. Session Versus Single-Baseline GPS Processing, *Proc. ION GPS-92*, Albuquerque, New Mexico, 16-18 September, 995-1004.
6. Dixon, T.H., Mao, A., Bursik, M., Heflin, M., Langbein, J., Stein, R. and Webb, F., 1997. Continuous Monitoring of Surface Deformation at Long Valley Caldera, California, with GPS, *Journal of Geophysical Research*, 102(B6), 12017-12034.
7. Han, S., 1997. *Carrier Phase-Based Long-Range GPS Kinematic Positioning*, PhD Dissertation, UNISURV S-49, School of Geomatic Engineering, The University of New South Wales, Sydney, Australia, 185pp.
8. Han, S. and Rizos, C., 1996. GPS Network Design and Error Mitigation for Real-Time Continuous Array Monitoring Systems, *Proc. ION GPS-96*, Kansas City, Missouri, 17-20 September, 1827-1836.
9. Hartinger, H. and Brunner, F.K., 2000. Development of a Monitoring System of Landslide Motions Using GPS, *Proc. 9th FIG Int. Symp. on Deformation Measurements*, Olsztyn, Poland, September 1999, 29-38.
10. Hudnut, K.W., Bock, Y., Galetzka, J.E., Webb F.H. and Young, W.H., 2001. The Southern California Integrated GPS Network (SCIGN), *Proc. 10th FIG Int. Symp. on Deformation Measurements*, Orange, California, 19-22 March 2001, 129-148.
11. Janssen, V., 2001. Optimising the Number of Double-Differenced Observations for GPS Networks in Support of Deformation Monitoring Applications, *GPS Solutions*, 4(3), 41-46.
12. Janssen, V., Roberts, C., Rizos, C. and Abidin, H.Z., 2001. Experiences with a Mixed-Mode GPS-Based Volcano Monitoring System at Mt. Papandayan, Indonesia, *Geomatics Research Australasia*, 74, 43-58.
13. IPS, 2000. Space Weather and Satellite Communications, http://www.ips.gov.au/papers/richard/space_weather_satellite_communications.html, 7pp.
14. Klobuchar, J.A., 1996. Ionospheric Effects on GPS, in: Parkinson, B.W. and Spilker, J.J. (Eds.), 1996. *Global Positioning System: Theory and Applications Volume I*, Progress in Astronautics and Aeronautics, 163, American Institute of Aeronautics and Astronautics, Washington, 485-515.
15. Meertens, C., 1999. Development of a L1-Phase GPS Volcano Monitoring System – Progress Report for the Period 12 August 1998 – 15 May 1999, http://www.unavco.ucar.edu/~chuckm/l1prog99.pdf.
16. Mendes, V.B., 1999. *Modeling the Neutral-Atmosphere Propagation Delay in Radiometric Space Techniques*, PhD Dissertation, Dept. of Geodesy & Geomatics Eng. Tech. Rept. No. 199, University of New Brunswick, Fredericton, Canada, 353pp.
17. Ogaja, C., Rizos, C., Wang J. and Brownjohn, J., 2001. A Dynamic GPS System for On-line Structural Monitoring, *Proc. Int. Symp. on Kinematic Systems in Geodesy, Geomatics & Navigation (KIS 2001)*, Banff, Canada, 5-8 June, 290-297.
18. Rizos, C., 1997. *Principles and Practice of GPS Surveying*, Monograph 17, School of Geomatic Engineering, The University of New South Wales, Sydney, Australia, 555pp.
19. Rizos, C., Han, S. and Chen, H.Y., 1998. Carrier Phase-Based, Medium-Range, GPS Rapid Static Positioning in Support of Geodetic Applications: Algorithms and Experimental Results, *Proc. Spatial Information Science & Technology (SIST'98)*, Wuhan Technical University of Surveying and Mapping, Wuhan, P.R. China, 13-16 September, 7-16.

20. Rizos, C., Han, S., Ge, L., Chen, H.Y., Hatanaka, Y. and Abe, K., 1999. Low-Cost Densification of Permanent GPS Networks for Natural Hazard Mitigation: First Tests on GSI's GEONET Network, *Earth, Planets and Space (EPS), Special Volume on Proc. of the Int. Symp. on GPS – Applications to Earth Sciences & Interaction with other Space Geodetic Techniques*, Tsukuba, Japan, 18-22 October, 6pp.
21. Roberts, C., 2002. *A Continuous Low-Cost GPS-Based Volcano Deformation Monitoring System in Indonesia*, PhD Dissertation, School of Surveying and Spatial Information Systems, The University of New South Wales, Sydney, Australia, 287pp.
22. Saalfeld, A., 1999. Generating Basis Sets of Double Differences, *Journal of Geodesy*, 73, 291-297.
23. SCIGN, 2001. http://www.scign.org/
24. Seeber, G., 1993. *Satellite Geodesy*, de Gruyter, Berlin, Germany, 531pp.
25. Shimada, S., Fujinawa, Y., Sekiguchi, S., Ohmi, S., Eguchi, T. and Okada, Y., 1990. Detection of a Volcanic Fracture Opening in Japan Using Global Positioning System Measurements, *Nature*, 343, 631-633.
26. SOPAC, 2001. http://sopac.ucsd.edu/cgi-bin/SCOUT.cgi
27. Tsuji, H., Hatanaka, Y., Sagiya, T. and Hashimoto, M., 1995. Coseismic Crustal Deformation from the 1994 Hokkaido-Toho-Oki Earthquake Monitored by a Nationwide Continuous GPS Array in Japan, *Geophysical Research Letters*, 22(13), 1669-1672.
28. Wanninger, L., 1999. The Performance of Virtual Reference Stations in Active Geodetic GPS-Networks under Solar Maximum Conditions, *Proc. ION GPS-99*, Nashville, Tennessee, 14-17 September, 1419-1427.
29. Wong, K.-Y., Man, K.-L. and Chan, W.-Y., 2001. Monitoring Hong Kong's Bridges – Real-Time Kinematic Spans the Gap, *GPS World*, 12(7), July 2001.
30. Wu, J.T., 1994. Weighted Differential GPS Method for Reducing Ephemeris Error, *Manuscripta Geodaetica*, 20, 1-7.